J Electroceram (2009) 23:242–247
DOI 10.1007/s10832-007-9412-z

A newly designed chopper for pyroelectric infrared sensor by using a dome-shaped piezoelectric linear motor (DSPLM)

Yoon Man-Soon · Heo Sung-Moo · Ur Soon-Chul

Received: 30 May 2007 / Accepted: 27 December 2007 / Published online: 12 March 2008

Abstract In an attempt to develop a compact and simple structured chopper for a PIR (Pyroelectric Infrared Ray) sensor, a smart ultrasonic linear motor was introduced for a new solid state chopper. The actuating component contains a dome-shaped monolithic piezoelectric ceramic fabricated using PIM. Dome-shaped piezoelectric actuator (DSPA) parts having two different diameters, 5 mm and 8 mm, each with the same curvature radius of 10 mm, were fabricated using powder injection molding (PIM). Dynamic characteristics of the linear motors were evaluated. As a result, it was found that the maximum tip displacements in the Φ 8 and Φ 5 samples were 700 and 300 nm, respectively. To measure the output characteristics as a function of chopping period, the changes of output signals at various chopping periods (1 to 3 s) were observed by applying stationary infrared rays. The observed pulse signal voltages were a value of 1.7 to 2.2 V. As the intermitting period increased, output signals decreased as much as 0.5 V. When the DSPLM chopper is operated at room temperature after removing the IR source, the average noise output voltage was 0.3V, resulting in a one-sixth lower value compared with the output voltage when the infrared rays were incident. These results indicated that the signal-to-noise ratio has available values within 5.4 to 7.2. Moreover, it was shown that the power consumption was less than 1 watt when the DSPLM was in operation. Therefore, a module of the continuously detectable PIR sensor that was compact in size with reduced power consumption and high reliability was successfully realized using the DSPLM chopper.

Keywords Dome-shaped · Piezoelectric · Pyroelectric · Infrared · Sensor

Y. Man-Soon · H. Sung-Moo · U. Soon-Chul (✉)
Department of Materials Science and Engineering/Research Center for Sustainable Eco-Devices and Materials (ReSEM), Chungju National University,
Chungbuk 380-702, Korea
e-mail: scur@chungju.ac.kr

1 Introduction

In recent years, pyroelectric infrared-ray sensors have been utilized in a broad range of fields for a variety of purposes such as food temperature measurements during cooking in electronic ovens, detection of human body locations in certain areas cooled with air conditioners, light switch controls, and security systems.

The PIR sensors take advantage of pyroelectric effects obtainable with pyroelectric materials such as $LiTaO_3$ single crystal or PZT polycrystal [1, 2].

Pyroelectric materials have spontaneous polarization and always produce electric charges on surfaces. However, pyroelectric materials are kept electrically neutral in their stationary objects in an atmosphere where the electric charges are coupled with charges in the atmosphere [3]. When infrared rays are incident on pyroelectric materials, their temperatures are changed, and then destroying or changing the neutral state of the electric charges produced on the surfaces, thereby measuring quantities of incident infrared rays is possible. Generally, the incident infrared rays of PIR sensors should be periodically interrupted by means of a chopper which consists of a motor and revolving plate, in order to continuously measure the constant temperature of the portion to be detected [4]. However, since the conventional chopper is relatively large with high electric consumption and low reliability, a compact sized solid-state chopper is required.

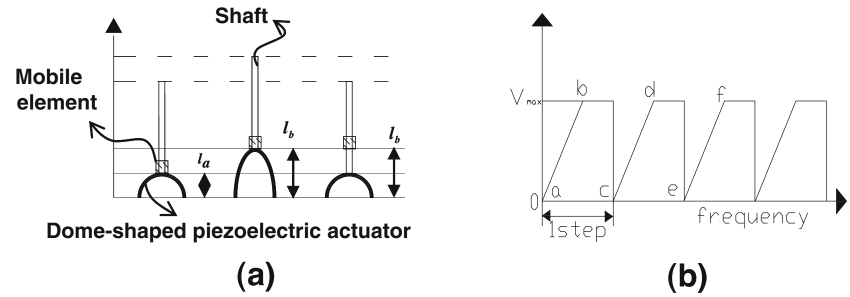

Fig. 1 The principle of inertia displacement (**a**) and (**b**) saw tooth electrical potential

This study aims to propose and develop a newly designed chopper for a PIR sensor by using a dome-shaped piezoelectric linear motor (DSPLM) with a compact structure, higher reliability, and lower electric power consumption [5].

To address these problems, the displacement characteristics of a dome-shaped piezoelectric actuator (DSPA) were measured using a non-contacting displacement sensor. The operation characteristics of the PIR sensor, since stationary infrared rays were intermitted by the newly developed solid-state chopping system, were investigated and evaluated.

2 Experimental procedure

2.1 Operation principle of a dome-shaped piezoelectric linear motor

The linear motion of the newly developed linear motor is operated by the principle of inertia displacement, which can be explained by a saw tooth electrical potential as shown in Fig. 1(a) and (b). Fig. 1(a) shows the motions of a mobile element induced by the DSPA. When a mobile element locates at position l_a in Fig. 1(a), the electric potential is not applied, represented as “a” position in Fig. 1(b), which is called the initial state. During a gentle rise in the drive signal applied to the DSPA [a–b position in Fig. 1(b)], the DSPA will slowly expand. Accordingly, the mobile element coupled with the drive shaft by friction will move to the upper direction, represented as position l_b in Fig. 1(a).

As the electric potential suddenly falls to the “c” position in Fig. 1(b), which is the minimum electric potential, the DSPA quickly contracts towards the down direction. However, the mobile element remains in its second position “l_b” since its inertial force keeping it there exceeds the frictional coupling force. Therefore, the mobile element moves in position with the distance of l_b–l_a. Consequently, the mobile element will move repeatedly when the drive signal is applied for a desired number of times. If the slope of the saw tooth in the electrical potential is reversed, the direction of the mobile element would be reversed. It can be said that the DSPLM proposed here realizes the principle of inertial displacement. Moreover, it provides much higher reliability than multi-layer or bimorph-type actuators [6, 7].

2.2 Structure of chopper combined with DSPLM

Figure 2 shows an exemplary construction of a DSPLM and chopper. The DSPLM consists of four parts, the actuating component, drive shaft, mobile element and chopping plate. The actuating component contains a dome-shaped monolithic piezoelectric ceramic fabricated using PIM. The displacement of the actuating component is transferred to the drive shaft. The shaft is located at the center of the dome-shaped piezoelectric actuator. The mobile element is coupled with the outer surface of the shaft bound by an elastomer made from silicone rubber. The frictional force can be controlled by the elastic force of silicon rubber. The chopping plate is coupled with the outer surface of the elastomer. As shown in Fig. 2, one end of chopping plate is manufactured into a rectangular shape in order to cover up the PIR sensor.

2.3 Experimental details

2.3.1 Sample preparation

A $0.04Pb(Sb_{0.5}Nb_{0.5})O_3$–$0.46PbTiO_3$–$0.5PbZrO_3$ composition, which is generally used for a bimorph actuator, was used to fabricate the piezoelectric devices. A preliminary study indicated that this composition is characterized by excellent dielectric/piezoelectric properties (d_{33}~550pC/N, $k_{33}^T \sim 1,450$, k_p=0.7 at room temperature) and high Curie

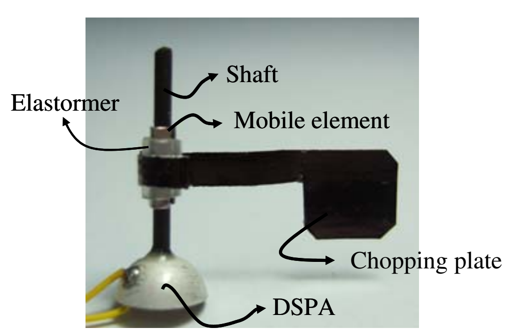

Fig. 2 An exemplary structure of Chopper combined with DSPLM

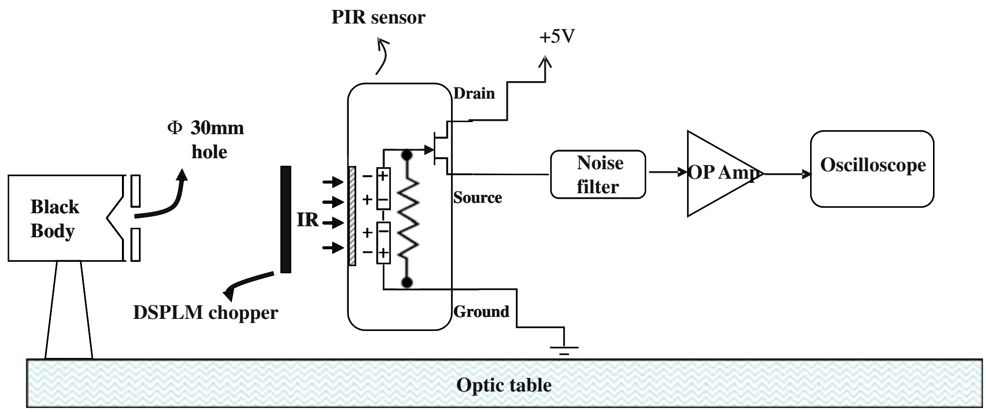

Fig. 3 Block diagram of the overall experimental system and a basic structure of the PIR sensor

temperature (T_c=320). In this experiment, DSPAs with diameters of 5 mm and 8 mm, with the same curvature radius of 10 mm and a thickness of 0.5 mm were fabricated using PIM. To evaluate the electromechanical properties, the sintered specimens were polished and electroded with silver paste (Metech Inc. no. 3288) fired at 650°C for 30 min, and then poled in a stirred silicone oil bath at 150°C by applying a dc electrical field of 2.5 kV/mm for 40 min.

2.3.2 Electromechanical properties

To measure the central tip vibration displacement of the DSPA at resonance frequency, a Micro Laser interferometer (Cannon, DS-80) was used as a non-contact displacement sensor. The applied voltage generated by the function generator (nF, WF 1943A) and high voltage amplifier (nF, HSA4052) was $50V_{o-p}$ at 72.4 and 109.2 kHz, respectively, and displacement signals were then measured using an oscilloscope (YOKOKAWA, DL 1620). To gain the power consumption of the DSPLM, the driving voltage and current of the DSPLM are measured by voltage (Tektronix, P5200) and a 10:1 current probe (Tektronix, P6021).

2.3.3 The effect of chopping periods on the output signal of a PIR sensor

The system shown in Fig. 3 was made to observe the characteristics of infrared detection of a chopper using a DSPLM. Infrared rays were emitted through a 30 mm diameter hole installed in front of a black body (ISOTECH, Model 9116) that kept the temperature of 310 K similar with the temperature of the human body. The emitted IR was interrupted periodically by the DSPLM chopping plate connected with a driving circuit, and then the intermitted IR was incident on the PIR sensor (NICERA, dual-type sensor, Model SDA0254), which was 1 mm away from the chopping plate.

In order to measure a signal from the PIR sensor, 5V from a DC power source was supplied to the drain and ground terminals, and the signal produced from a source terminal was transmitted into OP AMP (LM324N) through

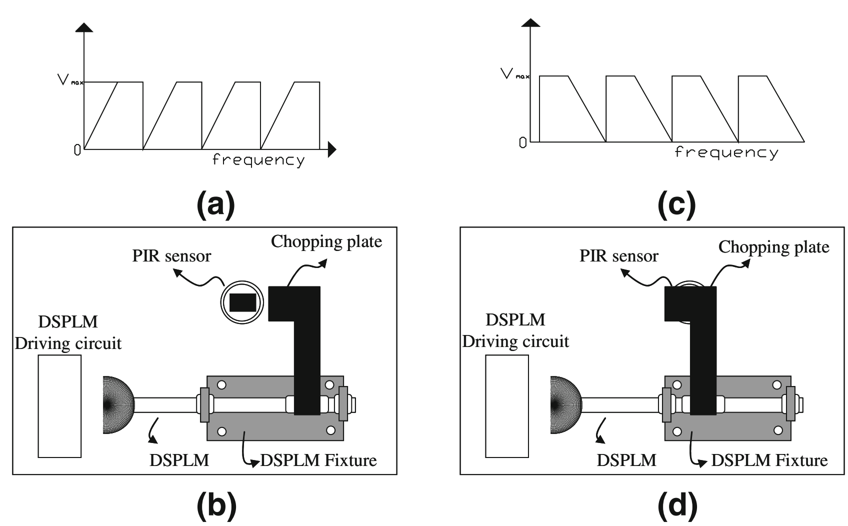

Fig. 4 DSPLM chopping system for intermitting IR: (**a**), (**c**) driving waveform, (**b**), (**d**) chopping plate direction

a noise filter and amplified 1,000 times. The gain of amplifier was designed for having a maximum value at 1 Hz. The amplified signals were measured and recorded by an oscilloscope. Fig. 3 also shows a basic structure of the PIR sensor. Since the PIR sensor used in the experiment is composed of two pyroelectric elements in series (opposed configuration), this sensor has low sensitivity to ambient temperature variation, vibration and optical noise.

To estimate the intrinsic characteristics of the PIR sensor, when the stationary IRs emitted from black body was incident on the PIR sensor which was sustained at room temperature, the output signal was observed and evaluated.

Figure 4 shows the DSPLM chopping system for intermitting stationary infrared rays incident upon the PIR sensor. The PIR sensor and DSPLM chopper were mounted on the same board. When a waveform like that shown in Fig. 4(a) was applied to the DSPLM, the chopping plate moved toward the right and the IR was incident on the PIR sensor as shown in Fig. 4(b). On the other hand, when a waveform such as in Fig. 4(c) was applied, the chopping plate moved toward the left and covered up the PIR sensor to block the IR. To measure the output characteristics as a function of chopping period, the operation period of the DSPLM chopper was set as shown in Fig. 5. T_1 and T_3 are the times during which the DSPLM chopper operates and the PIR sensor is completely opened and closed, respectively, and they are fixed at 0.2 s. On the other hand, T_2, T_4 are the holding times during which the PIR sensor is maintained in a completely opened and closed state, respectively, and are set to be the same time interval. The total time from T_1 to T_4 is defined as one period. The changes of output signals at various chopping periods (1 to 3 s) were observed by applying stationary infrared rays. Under the same chopping periods, the chopping noise signals of the PIR sensor were measured by operating the DSPLM chopper at room temperature after removing the infrared rays.

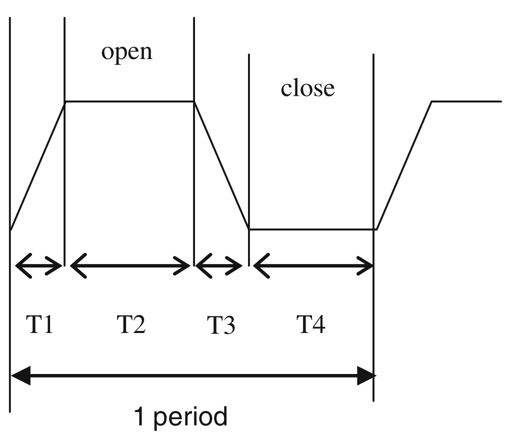

Fig. 5 The operation period of the DSPLM chopper

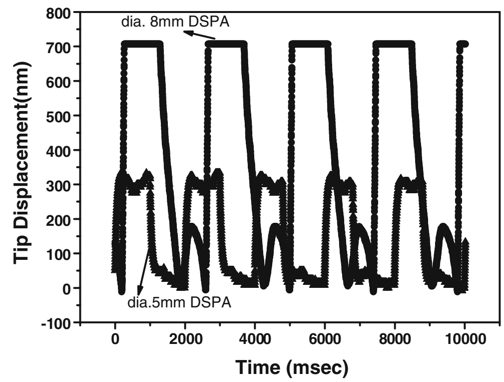

Fig. 6 The axial tip vibration displacements for different diameter of DSPA

3 Results and discussion

3.1 Maximum vibration displacement

The DSPA samples tested were 5 and 8 mm in diameter with the same thickness of 0.5 mm. Fig. 6 shows the axial vibration displacements of both samples measured with first resonance frequency and applied 50 V_{o-p}. These results indicate that the maximum tip displacements in the 8 Φ and 5 Φ samples are 700 and 300 nm, respectively. Note that the maximum tip displacement increases with the increasing diameter, as long as the samples are the same thickness and have the same curvature radius. It has been shown that the Φ 8 mm motor with dome-shaped piezoelectric part has a longer moving distance and higher load-resistance properties than the Φ 5 mm motor [5].

3.2 Operational characteristics of modulated PIR sensor

When the stationary IR emitted from black body was incident on the PIR sensor which was sustained at room temperature, the intrinsic output signal is as shown in Fig. 7.

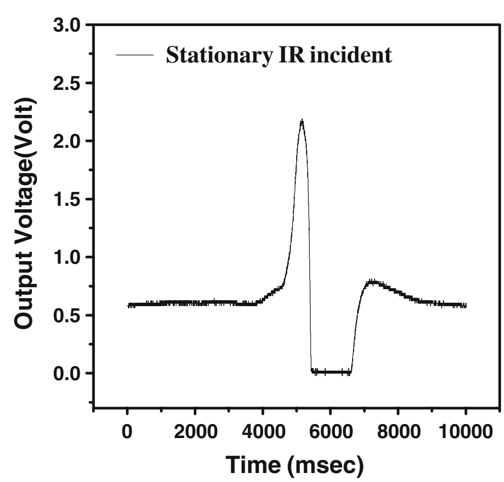

Fig. 7 The intrinsic output signal

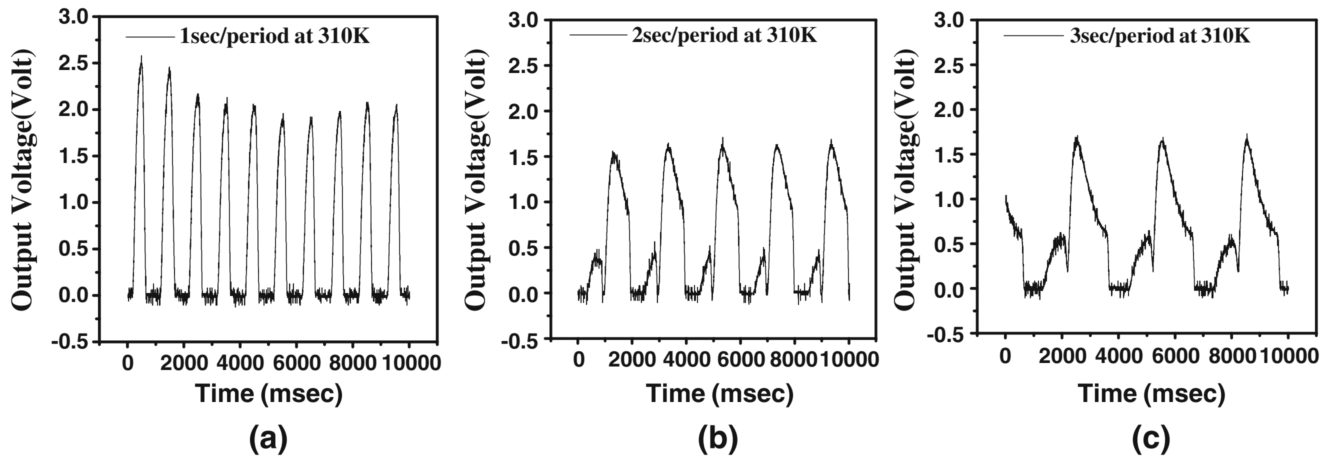

Fig. 8 Output signal responses for the PIR sensor as a function of various intermitting periods at stationary incident IR (310 K)

Based on 0.6 V, the output signals with the upper and lower peaks are detected. This phenomenon is a basic characteristic curve of the dual-element type PIR sensor. As shown in Fig. 3, since the PIR sensor was composed of two pyroelectric elements in series-opposed configuration, each element produces signals with a difference in phase when the IR is incident.

Meanwhile, as the infrared rays are kept at a stationary state, the output peaks disappear. However, when the constant incident infrared rays are intermitted periodically by the DSPLM chopper, output signal responses for the PIR sensor at various intermitting periods are as presented in Fig. 8(a)–(c).

These results indicate that the stationary infrared rays incident to the PIR sensor are effectively interrupted. Consequently, pulse signals with constant peak value are obtainable for the stationary infrared rays. Furthermore, Fig. 8 shows the changes of the output voltage curves when the intermitting period is increased from 1 to 3 s at intervals of 1 s. Comparing with the average maximum output voltage of a second period, those of 2 and 3 s periods decreased as much as 0.5 V. A typical experiment will measure the output of a sensor as a frequency is varied. In this experiment, the response of PIR sensor is given by the responsivity equation [8]:

$$V = \eta P_0 p \omega A \frac{R_t}{\sqrt{1+\omega^2\tau_t^2}} \frac{R_e}{\sqrt{1+\omega^2\tau_e^2}} \tag{1}$$

Where η is the emissivity of surface of sensor, P_0 is the peak value of the modulation of the infrared ray, p is the pyroelectric coefficient, ω is the angular frequency of radiation modulation, A is the sensor area, R_t and R_e are the thermal and electric resistances and τ_t and τ_e are the thermal and electrical resistances. According to the model proposed by Benjamin and Armitage [9], at very low frequencies, Eq. 1 reduces to a simple form where frequencies the voltage is proportional to ω (and at high frequencies the voltage is proportional to $1/\omega$). Since the intermitting period increases from 1 to 3 s, modulation frequency decrease from 1 to 0.33 Hz. Therefore, average output voltage was decreased as increasing intermitting period.

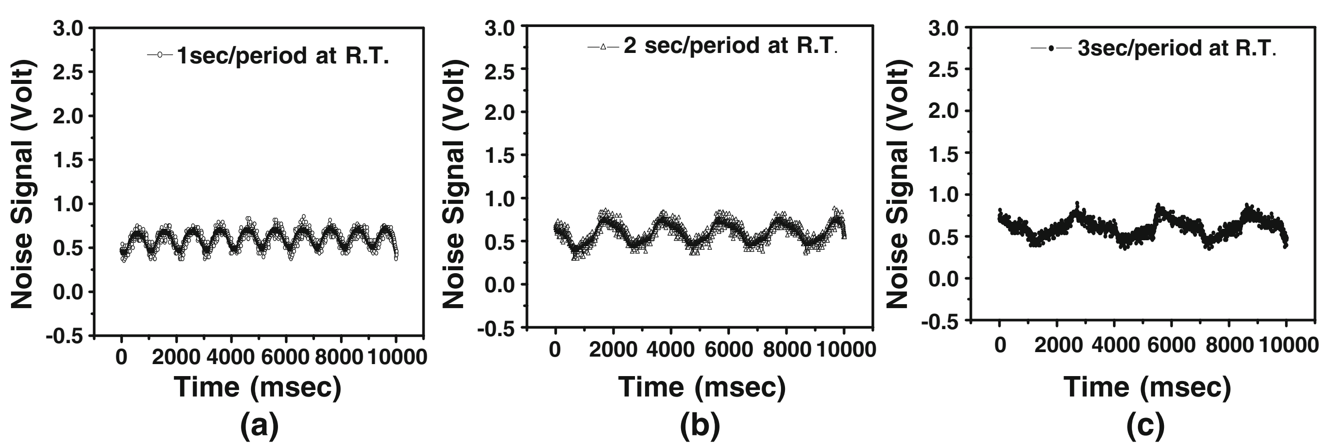

Fig. 9 The chopping noise when the DSPLM chopper is operated at room temperature after removing the IR source; (**a**) 1 s/period, (**b**) 2 s/period, (**c**) 3 s/period

As the intermitting period increases, two separated signals are obviously represented. When a chopping period is adequately longer than the thermal time constant of the pyroelectric elements in the PIR sensor, different signals generated from the two pyroelectric elements are separately represented as shown in Fig. 8(b) and (c). However, as chopping period is shorter than the thermal time constant, the separated peaks overlap each other as shown in Fig. 8(a).

Figure 9 shows the chopping noise when the DSPLM chopper is operated at room temperature after removing the IR source. From the results, the average noise output voltage was 0.3 V, resulting in a one-sixth lower value compared with the output voltage when the infrared rays were incident. These results indicate that the signal-to-noise ratio has available values within 5.4 to 7.2. Moreover, when the DSPLM was in operation, the power consumption was less than 1 W.

As discussed previously, the DSPLM chopping system clearly demonstrates that stationary infrared rays are effectively intermitted. Therefore, a module of the continuously detectable PIR senor that was small in size with reduced power consumption and high reliability was successfully realized using the DSPLM chopper.

4 Conclusions

To develop a compact and simple structured chopper for a PIR sensor, a smart ultrasonic linear motor was introduced for a new solid state chopper. Dome-shaped piezoelectric actuator (DSPA) parts having two different diameters, 5 and 8 mm, each with the same curvature radius of 10 mm, were fabricated using powder injection molding (PIM). Dynamic characteristics of the linear motors were evaluated. It has been shown that the Φ 8 mm motor with dome-shaped piezoelectric part has a longer moving distance and load-resistance properties than those in the Φ 5 mm motor. The dome-shaped piezoelectric actuator samples tested revealed that the maximum tip displacements in the 8 Φ and 5 Φ samples were 700 and 300 nm, respectively. When infrared rays close to the temperature of the human body were stationary incident on the PIR sensor from the blackbody, pulse signals with constant peak value of 1.7 to 2.2 V were observed, and the average noise output voltage was 0.3 V, resulting in a one-sixth lower value compared with the output voltage when the infrared rays were incident, regardless of the intermitting period. Thus, the signal-to-noise ratio obtained has a value of 5.4 to 7.2. Moreover, it was shown that the power consumption was less than 1 watt when the DSPLM was in operation. Therefore, a module of the continuously detectable PIR sensor that was small in size with reduced power consumption and high reliability was successfully realized using the DSPLM chopper.

Acknowledgement This research was supported by the Program for the Training of Graduate Students in Regional Strategic Industries and Regional Innovation Center (RIC) Program which was conducted by the Ministry of Commerce, Industry and Energy of the Korean Government.

References

1. T.M. Hussain, A.M. Baig, T.N. Saadawi, S.A. Ahmed, Infrared pyroelectric sensor for detection of vehicular traffic using digital signal processing techniques IEEE Trans. Veh. Technol. **44**, 683 (1995)
2. N. Yoshiike, K. Morinaka, K. Hashimoto, M. Kawaguri, 360° type human information sensor Sens. Actuators A. **77**, 199 (1999)
3. A.J. Moulson, J.M. Herbert, *Electroceramics* (Wiley, England, 2003), p. 423
4. E.E. Russell, F.G. Brown, R.A. Chandos, W.C. Fincher, L.F. Kubel, A.A. Lacis, L.D. Travis, Galileo photopolarimeter/radiometer experiment J. Electroceram **60**(1–4), 531 (1992)
5. M.S. Yoon, Y.G. Choi, S.C Ur, Displacement properties of newly developed 3-Dimensional piezoelectric actuator at various AC frequencies Mat. Sci. Forum **534**, 1441 (2007)
6. K. Kawabe, Sakai (Minolta Co., Ltd.), Actuator driving circuit, an actuator driving device, and an actuator driving method, US patents 6 320 298 B1, 20 November (2001)
7. S. Borodin, J.D. Kim, H.J. Kim, P. Vasiljev, S.J. Yoon, Nano-positioning system using linear ultrasonic motor with shaking beam Journal of Electroceramics. **12**(3), 169 (2004)
8. S.G. Porter, A brief guide to pyroelectric devices Ferroelectrics **33**, 193 (1981)
9. K.D. Benjamin, A.F. Armitage, R.B. South, Harmonic errors associated with the use of choppers in optical experiments Measurement. **39**, 764 (2006)